

RSC Advances



This is an *Accepted Manuscript*, which has been through the Royal Society of Chemistry peer review process and has been accepted for publication.

Accepted Manuscripts are published online shortly after acceptance, before technical editing, formatting and proof reading. Using this free service, authors can make their results available to the community, in citable form, before we publish the edited article. This *Accepted Manuscript* will be replaced by the edited, formatted and paginated article as soon as this is available.

You can find more information about *Accepted Manuscripts* in the [Information for Authors](#).

Please note that technical editing may introduce minor changes to the text and/or graphics, which may alter content. The journal's standard [Terms & Conditions](#) and the [Ethical guidelines](#) still apply. In no event shall the Royal Society of Chemistry be held responsible for any errors or omissions in this *Accepted Manuscript* or any consequences arising from the use of any information it contains.

precisely, C-terminal telopeptide of collagen type II (CTX-II),⁷ cartilage oligomeric proteins (COMPs),⁸ matrix metalloproteinases^{9,10} and also hYKL-39¹¹⁻¹³ were recognized as biomarkers for OA, through a combination of molecular biology, biochemistry and pathology. The routine method for detecting biomarkers in body fluids is the optical enzyme-linked immunosorbent assay (ELISA), which requires antibody against the indicator molecule and an enzyme-labelled secondary antibody for signal generation.

Detection of OA biomarkers using techniques other than ELISA is possible but has rarely been attempted. Examples are optical CTX-II and COMP microfluidic assays that work with antibody-conjugated fluoro-microbeads as functional components.^{14,15} For COMP an immunochromatographic strip test, with gold nanoparticle-linked biomarker antibody immobilized on the sensing surface, was also reported.¹⁶ To promote electrochemical signalling as an option for signal transduction in OA biomarker immunoassays we demonstrate here, for the first time, the suitability of flow-based capacitive immunosensing for reliable OA biomarker analysis. Because of experience in the preparation and structural and functional characterization of chitinase and chitinase-like proteins and also successful quantification of the cancer biomarker human chitinase-3-like protein 1 (hYKL-40) in blood serum,¹⁷ hYKL-39 was chosen as the biomarker in this proof-of-principle study. The requisite electrochemical immunosensors were produced by fixing anti-hYKL-39 to a thin but insulating self-assembling monolayer of thiourea/ dodecanethiol on gold electrodes. The concentration-dependent signal in hYKL-39 quantification was the exponentially decaying capacitive current response of completed hYKL-39 immunosensors to potential steps. The performance of capacitive hYKL-39 immunosensing was tested for the determination of the OA marker in 'spiked' samples spanning a pathologically relevant analyte concentration range, in lysates from various human cells and in synovial fluid samples from OA patients in a local clinic. Parallel assessments of duplicates of all these samples with conventional optical ELISA confirmed the data from the novel electrochemical hYKL-39 test, proving the validity of the methodology and promoting further applications for clinical osteoarthritis diagnosis. All relevant study details are presented hereafter.

2. Experimental

2.1 Chemicals and materials

Chemicals were of analytical grade and, unless otherwise specified, obtained from SM Chemical Supplies Co. Ltd. (Bangkok, Thailand) or Italmar Co. Ltd (Bangkok, Thailand). The ultrapure water for electrode cleaning and buffer preparation came from a reverse osmosis/deionization purification system and was passed through a cellulose nitrate membrane filter of pore size 0.20 μm (Whatman, GE Medical Systems Ltd., Bangkok, Thailand) before use. YKL-39 antigen and hYKL-39 antibody preparation and purification followed procedures as described in detail earlier by Ranok et al. (2013).¹³ Human cell lines used in this study were from the American Cell Culture

Collection (Manassas, VA). Disk-shaped Au electrodes were prepared from crystalline Au rods of 3 mm diameter and 1 cm length and Au of 99.9 % purity, obtained from a local gold shop (Tang Kim Heng Gold Shop, Nakhon Ratchasima, Thailand).

2.2 Capacitive hYKL-39 immunosensor preparation

Capacitive hYKL-39 immunosensors were made by a previously reported fabrication procedure.¹⁷⁻²⁰ The series of mechanical and electrochemical cleaning steps, amino-thiol monolayer formation and antibody immobilization by glutaraldehyde-assisted crosslinking is illustrated in the Supplementary Content in Figure S1. In brief, the exposed surface of the 3-mm-diameter gold disk working electrode (Au-WE) was first freed from surface dirt and polished by intense circular rubbing on soft polishing pads soaked with alumina slurries of decreasing particle size (5, 1 and finally 0.5 micron), then¹⁵ 15 min ultrasonication in water and drying in a stream of inert N_2 gas. Polished and dried electrodes were further electrochemically cleaned in 0.5 M H_2SO_4 with 25 repetitions of a 100 mV/s potential scan from 0 to + 1.5 V vs. an Ag/AgCl reference electrode. After rinsing in water and drying with N_2 , the cleaned gold disks were immersed in 250 mM thiourea in water for 24 h at room temperature to allow formation of the required dense, covalently bound molecular thiol layer. This was followed by rinsing with water and drying in air in preparation for step 3, the coupling of anti-hYKL-39 to amine functionalities in the surface-anchored thiourea molecules, by glutaraldehyde-directed crosslinking. Thiolated Au-WEs were kept at room temperature for 20 min in a 5% (v/v) glutaraldehyde (GA) solution in 10 mM sodium phosphate buffer (PBS) pH 7.0. GA-treated sensors were rinsed with water, placed upside down in a suitable holder and 20 μL of 1 mg/mL anti-hYKL-39 in PBS placed on the top disk face. Antibody coupling was allowed to take place overnight at 4°C and at completion the freshly modified sensor tips were thoroughly rinsed with PBS to remove reagent solution. Measurements of capacitive currents for hYKL-39 quantification require full insulation of the Au-WE, which is not usually achieved by simply coating with thiourea. Residual conductive gaps in the films can, however, be blocked with smaller thiols, so the anti-hYKL-39/glutaraldehyde/thiourea-modified Au-WEs were immersed for 20 min in a 10 mM solution of 1-dodecanethiol in ethanol. The success of the immunosensor preparation was checked by cyclic voltammetry of 5 mM potassium ferricyanide in 0.1 M KCl and electrochemical impedance spectroscopy (EIS) with a 5 mM mixture of ferro-/ferricyanide as redox probe in 25 mM PBS (pH 7.0).

2.3 Flow-based capacitive hYKL-39 quantification

Measurements of hYKL-39 with capacitive readout of antigen-antibody binding were executed in a microfluidic workstation as described in detail in an earlier publication¹⁷ and also by others.¹⁸⁻²⁰ System modules included a three-electrode potentiostat with its software and data acquisition system (E. 163/ED410, eDAQ, Australia), a three-electrode flow cell with

opposite slots for the anti-hYKL-39-modified gold working-electrode (Au-WE) and the Ag/AgCl reference electrode (RE) and stainless steel (SS) connectors for the buffer influx and outflow tubing (the outlet SS canal served also as counter electrode), a peristaltic pump (Miniplus 3, Gilson, USA) offering a constant flow of running buffer and a 6-port injection valve (Biologic MV-6, Bio-Rad, USA) for injections of μL -sized samples.

In electrochemical experiments gold disk electrodes with well-insulating thiol films behave as electrical capacitors; one capacitor plate is the charged Au-WE surface, the other is the layer of electrostatically attracted ions and the dielectric is the thiol film in between. The capacitor capacitance is inversely proportional to the dielectric thickness. Antibody fixation to the thiol layer and later antigen capture inserts these units between the electrode face and the ion plane forming the Helmholtz double layer, producing a thickness increase and a capacitance decrease. This effect provides a very sensitive quantification of the binding of antibody to antigen. Baseline capacitances, C , of thiol/anti-hYKL-39-modified Au-WEs and capacitance changes, ΔC , on binding of hYKL-39 to surface-anchored antibody can be quantified by the analysis of the exponentially decaying current (i) in response to repetitive 50 mV potential steps of 6.375 ms duration, before and after antigen exposure. The value of i as function of time is given by the expression:

$$\ln i(t) = \ln E/R_s - (1/R_s \times C) \times t \quad (1)$$

where t is the time elapsed after the potential step was applied, R_s the dynamic resistance of the recognition layer, and C the total capacitance at the sensor/electrolyte interface. Linear least-squares plotting of $\ln i(t)$ against t allows calculation of R_s , from the intercept of the regression line and the known value of E , and of C , from the slope. While buffer was passed continuously through the electrochemical cell, a typical sample measuring cycle used a sequence of 25 potential pulses for sensor capacitance assessments, one every minute. Usually, 10 pulses were applied before and 10 after sample injection. The last 5 pulses occurred after injection of regeneration solution. For all pulses, the current response allowed computation of corresponding C values, which, plotted versus time, gave the baseline, the change due to sample exposure, and baseline recovery after regeneration. The measured parameter was ΔC on hYKL-39 capture, the difference between the C value after antigen exposure and the baseline. As shown earlier,¹⁶⁻¹⁹ ΔC scales with the concentration of injected antigen and construction of a calibration curve allows target quantification. Exposure of used hYKL-39 immunosensors to acidic regeneration buffer releases the antibody and the detector can then be reused.

Optimization trials with the capacitive hYKL-39 immunosensing procedure - for details and the data please refer to the Supplementary Content - identified 25 mM phosphate buffer (pH 7.0), 3.2 mM HCl (pH 2.5), 100 $\mu\text{L}/\text{min}$ and 200 μL as optimal running buffer, regeneration solution, flow rate and injected sample volume, respectively. System calibration under optimal conditions revealed the analytical

dynamic range, sensitivity and detection limit. Calibrated capacitive hYKL-39 immunosensors were used to quantify analyte concentrations in Jurkat, U937 and 293t cell lysates and in synovial fluid samples that were provided by the Department of Clinical Pathology at Maharaj Nakhon Ratchasima Hospital, Nakhon Ratchasima, Thailand with the informed consent of patients with OA. However, synovial fluid from healthy individuals was not available from the hospital partner for desirable controls. All experiments in this study were performed in compliance with the relevant laws and institutional guidelines of Suranaree University of Technology and permitted by its Ethics Committee for Research Involving Human Subjects, which obeys international rules in reviewing and approving procedures involving humans and animals.

2.4 ELISA assay for hYKL-39 determination

50 μL of 0.5–500 $\mu\text{g}/\text{L}$ hYKL-39 in coating buffer (15 mM Na_2CO_3 , 35 mM NaHCO_3 , pH 9.6) were loaded into standard ELISA plate wells and the protein allowed to adsorb onto the well surfaces during overnight incubation at 4°C. Coating buffer removal was followed by 1 hour of exposure of the antigen-loaded wells to blocking buffer (2% skimmed milk in PBS, pH 7) at 25°C; this filled vacant protein-binding sites and prevented non-specific binding of antibody. After removal of blocking buffer wells were rinsed four times with 200 μL washing buffer (PBS with 0.05% Tween 20, pH 7.2, PBS-T) and then incubated for 1 hour at 25°C with 50 μL of anti-hYKL-39 (15 $\mu\text{g}/\text{L}$ in blocking buffer). Wells were then washed four times with 200 μL washing buffer and incubated for further 1 hour at 25°C with 50 μL of horseradish peroxidase-conjugated goat anti-rabbit IgG (GenScript USA Inc., Piscataway, NJ), the stock (1 mg/L) diluted 1:2000 in PBS, pH 7.2. Lastly, the plate was washed three times with 200 μL washing buffer. Colour was developed by addition of 100 μL 3,3',5,5'-tetramethylbenzidine standard reagent solution (TMB, Invitrogen, Frederick, CA) and then 15 min dark incubation at 25°C. The reaction was stopped by adding 100 μL of 1N HCl. The intensity of the developed colour was determined spectrophotometrically using a Biochrome Anthos MultiRead 400 Microplate Reader (Biochem, United Kingdom) at 450 nm.

3. Results and discussion

The protein hYKL-39 is often referred to as a pseudo-chitinase since it has structural and sequence similarity to bacterial chitinases, but although it binds chito oligosaccharides it has no catalytic activity.^{13,21} A distinctive feature of hYKL-39 is its potential as OA biomarker, and the possible benefits of analysis of hYKL-39 in body fluids for understanding the onset and progression of OA has led to the search for hYKL-39 detection schemes. As mentioned above, ELISA is the standard means of hYKL-39 quantification. Here we explored the feasibility of hYKL-39 analysis by capacitive immunosensing, a technique that was previously shown to work well for other disease biomarkers. We first describe hYKL-39 immunosensor preparation and then discuss the parameters of the proposed

capacitive immunosensor scheme for specific hYKL-39 detection. We then report hYKL-39 analysis in synovial joint fluid from OA patients and in cell lysate, which was used to prove real sample quantification capability and clinical applicability either as an independent quantification scheme or as a novel auxiliary reference tool for the validation of measures obtained by standard optical ELISA screening.

3.1 Quality checks of hYKL-39 immunosensor

Ferricyanide cyclic voltammograms (CVs) for a gold electrode at different stages of modification are shown in the Supplementary Content as Figure S2. At the bare gold surface, forward and backward potential scans produced symmetrical current traces, indicating reversible analyte oxidation and reduction. Decreases in the cathodic and anodic peak currents were observed after reaction of the working electrode with thiourea, then glutaraldehyde and finally anti-hYKL-39, but even after immobilization of the bulky antibody the modified gold electrode retained significant electrochemical activity. To abolish current flow completely and limit electrode activity virtually to capacitive behaviour, the sensor surface was treated in a final step with 1-dodecanethiol, a linear thiol that filled the gaps left between anchored antibody molecules and established the tight insulation required for successful operation of capacitive immunosensing. The attainment of a proper interface for capacitive immunosensing was evident in CVs showing current lines with no significant redox current waves and in EIS measurements with ferro/ferricyanide as redox probe, which produced Nyquist plots typical of coated electrodes (Supplementary Content, Figure S3).

3.2 Analytical performance of capacitive hYKL-39 immunosensing

Fig. 1A shows the typical response of hYKL-39 immunosensors when sample (here: 100 $\mu\text{g/L}$ hYKL-39 in running buffer) is injected and the sensor capacitance, C , is recorded as a function of time. The two hYKL-39 additions produced well-defined stepped increases in C , indicating efficient capture of the antigen by immobilized anti-hYKL-39. Regeneration between individual injections effectively restored the baseline capacitance signal and the size of the capacitance change agreed well for the two additions. To identify the linear calibration range, hYKL-39 standard solutions of 1 ng/L to 10 mg/L were quantified by the immunosensor system, using the optimal condition parameter set. A typical calibration curve is shown in Figure 1B, a plot of the capacitance change, normalized to the geometric sensor area, against the logarithm of hYKL-39 concentration. Triplicate measurements of all analyte concentrations showed linearity of the signal response between 0.1 $\mu\text{g/L}$ and 1000 $\mu\text{g/L}$; the linear regression line drawn by standard software followed the equation $y = (16.12 \pm 0.44) \log(x) + (137.2 \pm 2.45)$ with a correlation coefficient of 0.99. As expected for binding to an immunosensor surface with a fixed number of adsorbed antibody molecules, the capacitance change in response to increasing antigen concentrations reached a plateau, here at concentrations above 1 mg/L. The limit of detection (signal-to-noise = 3) of capacitive hYKL-39 electroanalysis was 0.074 \pm

0.02 $\mu\text{g/L}$. Two hYKL-39 homologues, hYKL-40 and hAMCase (human acidic mammalian chitinase), were tested in the capacitive immunosensor system for cross-reactivity in the concentration range used for hYKL-39 (1 ng/L to 10 mg/L). Neither antigen produced a significant signal change over the concentration range tested (Fig. 1B). Interference even by closely related proteins could thus be excluded.

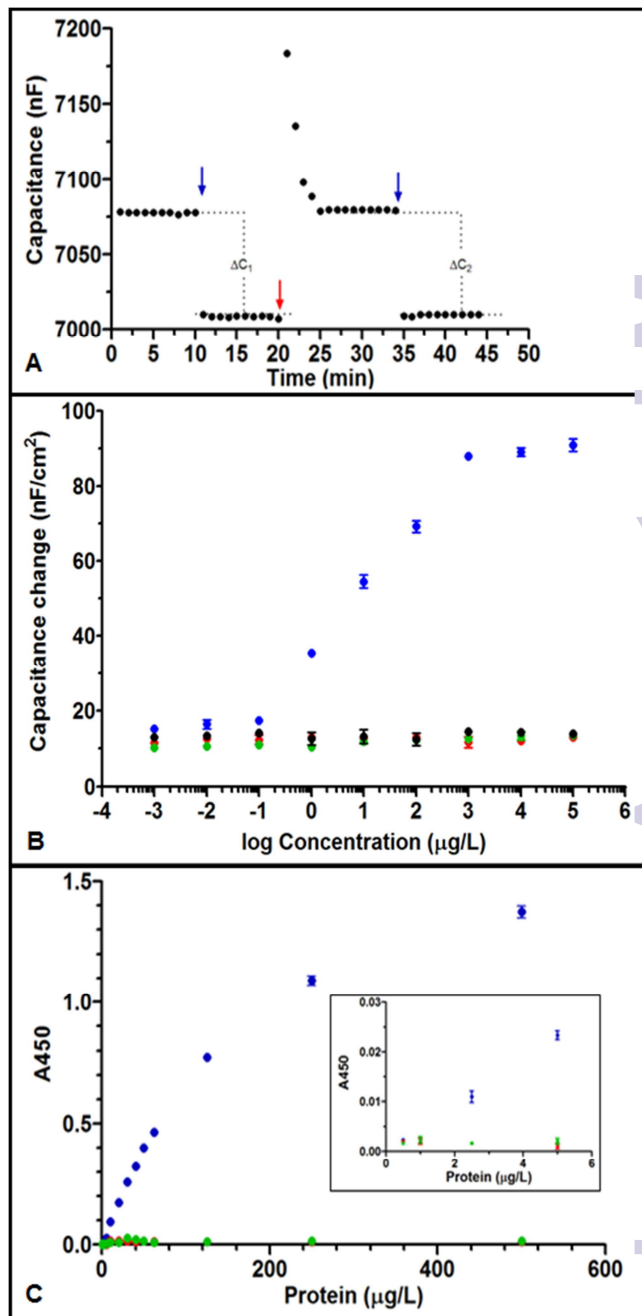


Fig 1. (A) Capacitance response of anti-hYKL-39-modified electrode. The baseline signal of the carrier buffer is initially recorded. 1st injection of 100 $\mu\text{g/L}$ of hYKL-39 (left blue arrow) triggered antigen binding and a decrease of capacitance (ΔC_1). Injection of the regeneration buffer (red arrow) removed hYKL-39 from the immunosensor surface and the capacitance returned to initial baseline. 2nd injection of 100 $\mu\text{g/L}$ of hYKL-39 (right blue arrow) produced capacitance change ΔC_2 . (B) Concentration dependence of the capacitance change for a hYKL-39 immunosensor elicited by hYKL-39 (blue curve) and hYKL-40 (red curve) and hAMCase (green curve) exposure. (C) Enzyme-linked immunosorbent assay (ELISA) of hYKL-39. Binding of anti-hYKL-39 IgG (50 μL , 15 $\mu\text{g/L}$) to different amounts of immobilized hYKL-39 (blue trace), hYKL-40 (red trace) and hAMCase (green trace). The inset is a zoom of the signal response at low concentration of the antigens.

The specificity of the anti-hYKL-39 serum was also confirmed with a standard optical ELISA experiment. Figure 1C shows binding of the hYKL-39 antibody to its target hYKL-39 and the reaction with hYKL-40 and hAMCase, for concentrations up to 500 $\mu\text{g/L}$. For hYKL-39 (blue trace) triplicate recordings of the absorbance signal for the distinct biomarker levels showed linearity from 2.5 - 125 $\mu\text{g/L}$, with a regression line correlation coefficient of 0.99 and pronounced levelling of the response at higher concentrations, typical of specific antibody-antigen interaction. In contrast hYKL-40 (red trace) and hAMCase (green trace) generated no signal above background level, excluding their recognition by anti-hYKL-39.

Obviously, the linearity of the electrochemical hYKL-39 screen extends at the upper and lower ends beyond those of the optical assay. The notably improved lower limit of linear response is a particular asset of the new procedure, as the OA biomarker can be quantified at concentrations beyond the reach of current ELISA. Detection closer to the onset of joint cartilage destruction thus is feasible and may permit better defect monitoring and control.

3.3 Signal stability of capacitive hYKL-39 immunosensing

Signal reproducibility and sensor stability over an extended time are crucial for analytical laboratory applications. The hYKL-39 immunosensors were therefore tested in the flow cell by monitoring, over 4 days, the capacitance changes for 57 sequential injections of 10 $\mu\text{g/L}$ hYKL-39. At the end of each measuring cycle 200 μL of 3.2 mM HCl was injected for sensor regeneration. The stability of the sensor was assessed from plots of the capacitance change recovery ($(\Delta C_{\text{injection \#(n+1)}}/\Delta C_{\text{injection \#n}}) \times 100$) vs. injection number. An example of such a trace is shown as Supplementary Figure S11. For 49 sample injections the regeneration treatment was sufficient to maintain the response of a hYKL-39 sensor within 95% of the capacitance change for first antigen exposure; with subsequent sample injections, however, the response declined. Apparently, the electrode coating is able to withstand the mechanical impact of the buffer flow and the cyclic variations in the chemical environment from running to regeneration buffer for several days.

3.4 Capacitive and ELISA hYKL-39 immunosensing in test samples

The measured capacitance and absorbance changes for individual model samples spiked with hYKL-39 in the concentration range 0.5–150 $\mu\text{g/L}$ was used to derive their OA biomarker content, from pre-determined calibration curves. The averaged data from triplicate measurements of each sample, together with the equivalent information from ELISA, are listed in Table 1. Both methods offered recoveries close to 100%; however in contrast to capacitive immunosensing, ELISA failed to quantify hYKL-39 in samples at the lowest and highest analyte concentrations tested, as expected from the differences in detection limit and linear range seen in the calibration trials discussed in section 3.2.

Table 1: Determination of hYKL-39 in model samples using capacitive immunosensor (n=3) and standard ELISA (n=3) quantification

hYKL-39 concentration ($\mu\text{g/L}$)	Detected hYKL-39 concentration ($\mu\text{g/L}$)			
	Immunosensor	% recovery	ELISA	% recovery
0.5	0.5 \pm 0.1	103.9 \pm 1.4	n. d.	n. d.
2.5	2.6 \pm 0.1	100.7 \pm 1.1	2.5 \pm 0.6	99.9 \pm 2.2
5.0	5.1 \pm 0.1	100.4 \pm 3.8	5.1 \pm 0.1	101.5 \pm 2.6
50.0	51.2 \pm 0.3	102.4 \pm 0.6	49.6 \pm 1.5	99.1 \pm 3.0
150.0	149.9 \pm 2.4	100.0 \pm 1.6	96.4 \pm 0.6	64.3 \pm 0.4

n. d. = not detected

3.5 Capacitive and ELISA hYKL-39 immunosensing in synovial fluid

The hYKL-39 concentrations in synovial fluids from four OA patients, donated by a local hospital, were determined by capacitive immunosensing and ELISA, in comparative trials. Both procedures were also used for hYKL-39 analysis in lysates from Jurkat, U937 and 293t cells. The choice of cells was based on the facts that Jurkat and U937 cell lysates have been reported to contain detectable levels of expressed hYKL-39 while the 293t cell line does not show hYKL-39 secretion. Jurkat and U937 lysates thus offered a physiological matrix that exposed the hYKL-39 immunosensors not only to their target but also to a mixture of other biomolecules with the potential to affect the analytical signal. Analyte-free 293t cell lysates, on the other hand, served as a useful negative control. Before biomarker quantification, samples were inspected by SDS-polyacrylamide gel electrophoresis (SDS-PAGE) and immunoblotting for hYKL-39 (Fig. 2). In each case Coomassie blue staining showed a band of the same mobility as pure hYKL-39 (Figure 2A, lane 8) in the four synovial fluids and in Jurkat and U937 cell lysates, which was confirmed by immunoblotting (Fig. 2B). Only 293t cell lysates produced no hYKL-39 signal in the immunoblot. hYKL-39 was expected in the synovial fluid of joints from positively diagnosed OA patients; its presence in the lysates of Jurkat and U937 cells, associated with innate and adaptive immune pathways, suggests that the protein may be involved in a defensive response to inflammation, however the exact mechanisms of this involvement are not yet clear and need further studies.

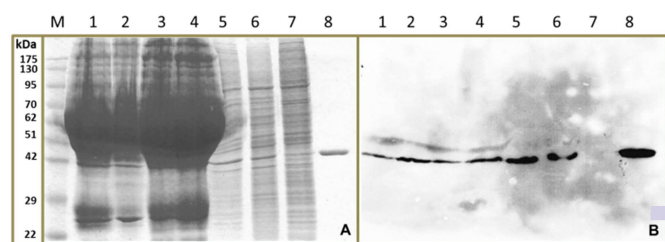


Fig. 2. Clinical samples and cell lysate electrophoresis on a 10% polyacrylamide SDS gel. Lane: M, protein markers; lanes 1–4, synovial fluid from osteoarthritis patients; lane 5, Jurkat cell lysate; lane 6, U937 cell lysate; lane 7, 293t cell lysate; lane 8, pure hYKL-39 (2 μg). (A) Coomassie-blue stained gel. (B) Immunoblot detected with anti-hYKL-39 polyclonal antibody (1:10,000 dilution).

Synovial fluids and cell lysates are complex mixtures; they were therefore diluted 10-fold with 25 mM phosphate buffer, pH 7.0 before immunosensor and ELISA analysis, in order to minimize matrix interference with signal generation. The superimposed capacitances plotted in the left part of the

traces in Fig. 3, up to 10 minutes, are the baseline values before sample injection, while the capacitances plotted in the left part of the traces in Fig. 3, up to 10 minutes, are the baseline values before sample injection when the hYKL-39 immunosensor is exposed to running buffer; 200 μL aliquots of the diluted samples were then injected. In agreement with immunoblot analysis of the samples, a significant capacitance decrease was observed with all pathological synovial fluids and for the Jurkat and U937 cell lysates; synovial fluid from healthy people was not available for analysis. Injection of 293t lysate, on the other hand, led to the same small capacitance decrease as the injection of measuring buffer alone. Capacitance changes with individual samples were used to derive their content of hYKL-39, from previously determined calibration curves. The averaged data from triplicate measurements of each sample, together with the same facts from ELISA, are listed in Table 2. Regarding accuracy, the results from electrochemical hYKL-39 immunosensing were not significantly different (by t-test) from those of the ELISA immunoassay, standard deviations being small for both methods. The synovial fluid samples from the four different OA patients varied in their hYKL-39 contents, again with good agreement between electrochemical immunosensor and optical ELISA. The observed difference may be a reflection of variation in OA status of the individuals providing the samples.

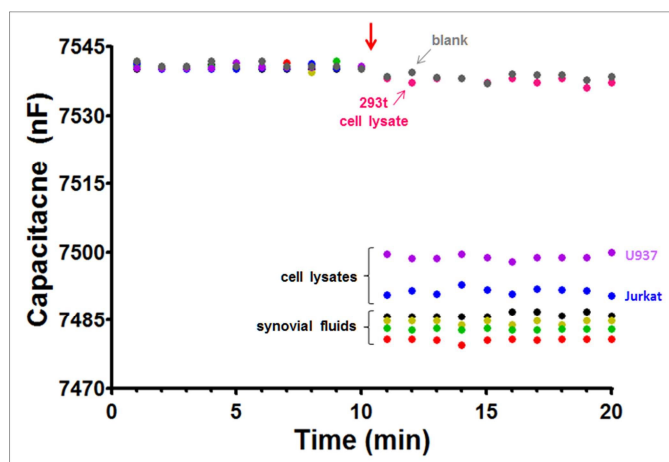


Fig 3. Cell lysate and synovial fluid analysis, by capacitive immunosensing. Sample injection is marked by a red arrow. A decrease in the sensor capacitance indicates the presence of hYKL-39, the concentration of which can be determined from the calibration curve.

The absence of hYKL-39 from 293t cell lysates allowed generation of samples with a genuine biological matrix but 'spiked' with known amounts of hYKL-39, for recovery measurements. hYKL-39 concentrations of 20 and 30 $\mu\text{g/L}$ were quantified and measurements with the capacitive immunosensor and control ELISA showed recoveries close to 100% in both cases (Table 3). Also included in Table 3 are trials with spiked synovial fluid samples. Based on a comparison with the values obtained for the non-spiked equivalents (Table 1) adequate recovery rates could be computed for the entire set of measurements and confirm the absence of confounding matrix effects. The observed competitive analytical performance in all the comparative trials reported suggest that

capacitive electrochemical immunosensing is a potentially valuable option for laboratories engaged in hYKL-39-based CA analysis, either as a reference tool or, especially for real sample levels down to 10-fold below the lower limit of linear range for ELISA testing, as a stand-alone approach.

Table 2: Determination of hYKL-39 in clinical samples and cell lysates using capacitive immunosensor (n=3) and standard ELISA (n=3) quantification

Sample	Detected hYKL-39 concentration ($\mu\text{g/L}$)	
	Immunosensor	ELISA
Synovial fluid # 1	59.4 \pm 2.4	58.3 \pm 3.4
Synovial fluid # 2	106.3 \pm 0.8	107.0 \pm 2.5
Synovial fluid # 3	68.1 \pm 1.3	67.7 \pm 1.2
Synovial fluid # 4	89.0 \pm 2.7	88.8 \pm 1.6
Jurkat	26.4 \pm 0.4	25.2 \pm 3.1
U937	10.6 \pm 0.3	9.8 \pm 0.8
293t	n. d.	n. d.

n. d. = not detected

Table 3: Determination of hYKL-39 in spiked clinical samples and 293t cell lysate using capacitive immunosensor (n=3) and standard ELISA (n=3) quantification

Spiked concentration ($\mu\text{g/L}$)	Detected concentration ($\mu\text{g/L}$)			
	Immunosensor ($\mu\text{g/L}$)	Recovery (%)	ELISA ($\mu\text{g/L}$)	Recovery (%)
Synovial fluid#1 + 50 $\mu\text{g/L}$	109.1 \pm 0.1	99.1 \pm 0.1	110.6 \pm 1.2	101.1 \pm 1.2
Synovial fluid#2 + 50 $\mu\text{g/L}$	155.1 \pm 1.0	99.2 \pm 0.6	156.7 \pm 0.8	99.8 \pm 0.4
Synovial fluid#3 + 50 $\mu\text{g/L}$	118.4 \pm 0.6	100.3 \pm 0.5	118.7 \pm 1.2	100.8 \pm 0.8
Synovial fluid#4 + 50 $\mu\text{g/L}$	139.6 \pm 0.4	100.4 \pm 0.3	141.6 \pm 1.2	102.0 \pm 0.7
293t + 20 $\mu\text{g/L}$	20.2 \pm 0.4	100.8 \pm 2.2	20.5 \pm 0.5	102.4 \pm 1.8
293t + 30 $\mu\text{g/L}$	29.7 \pm 0.2	99.1 \pm 0.7	30.4 \pm 0.5	101.2 \pm 1.2

The strongest argument for choosing the electrochemical over the optical strategy is the approximately 30-fold lower detection limit, as this would facilitate recognition of osteoarthritic joint degradation close to onset of the disease, when analyte levels are expected still to be very low. Simplicity, the low cost of instrumentation, convenience in operation, the portability of the small apparatus and the feasibility of fully automated measurements are additional features that make capacitive biosensing as described herein a recommendation for in-vitro hYKL-39 determinations in body fluids and cell lysates.

4. Conclusions

Attachment of an antibody directed against hYKL-39, a biomarker for osteoarthritis, to gold disk electrodes produced immunosensors that could measure sensitively the changes in capacitance on antibody-antigen binding, by analysis of current traces after the application of potential step. Capacitive hYKL-39 immunosensing had a wider linear response range and, more importantly, a lower detection limit than optical ELISA, which is currently the sole methodology for analysis of the biomarker in clinical and research laboratories. In synovial fluid from four different osteoarthritis patients the

electrochemical screen detected and quantified hYKL-39 with values in accordance with those from routine ELISA. The quality of the analytical performance of this first non-optical hYKL-39 assay and the general benefits of electrochemical equipment - low cost, simplicity and ease of operation are offered together with the feasibility of automation, miniaturization, and portability - make capacitive hYKL-39 immunosensing worth further exploration, in the wide field of osteoarthritis research.

Acknowledgements

Wethaka Chaocharoen is grateful for grant CHE510767 from The Office of the Higher Education Commission, Thailand and the program "Strategic Scholarships for Frontier Research Network for the Ph.D. Program, Thai Doctoral degree". Supporting funds came also through a Suranaree University of Technology (SUT) grant to Wipa Suginta and Albert Schulte (SUT1-102-57-24-01) and budget allocations to the Biochemistry - Electrochemistry Research Unit. Sincere thanks go to Dr. David Apps, Biochemistry Reader (retired), Centre for Integrative Physiology, Edinburgh University, Scotland for his critical manuscript reading and language improvement. We also acknowledge the support in general laboratory issues of the Biochemistry Laboratory of SUT's Center for Scientific and Technological Equipment and kind advice of Panote Thavarungkul and colleagues from the Trace Analysis and Biosensor Research Center, Prince of Songkhla University, Thailand in questions about capacitive immunosensing.

References

1. S. Glyn-Jones, A. J. R. Palmer, R. Agricola, A. J. Price, T. L. Vincent, H. Weinans and A. J. Carr, *Lancet*, 2015, **386**, 376-387.
2. S. Sovani and S. P. Grogan, *Orthop Nurs.*, 2013, **23**, 25-36.
3. M. Lotz, J. Martel-Pelletier, C. Christiansen, M. L. Brandi, O. Bruyère, R. Chapurlat, J. Collette, C. Cooper, G. Giacobelli, J. A. Kanis, M. A. Karsdal, V. Kraus, W. F. Lems, I. Meulenbelt, J. P. Pelletier, J. P. Raynaud, S. Reiter-Niesert, R. Rizzoli, L. J. Sandell, W. E. Van Spil and J. Y. Reginster, *Ann Rheum Dis.*, 2013, **72**, 1756-1763.
4. F. J. Blanco, *Osteoarthritis Cartilage*, 2014, **22**, 2025-2032.
5. M. F. Hsueh, P. Önnerfjord and V. B. Kraus, *Matrix Bio.*, 2014, **39**, 56-66.
6. M. Ishijima, H. Kaneko and K. Kaneko, *Ther. Adv. Musculoskelet. Dis.*, 2014, **6**, 144-153.
7. S. J. Kim, Y. M. Park, B. H. Min, D. -S. Lee and H. C. Yoon, *BioChip J.*, 2013, **7**, 399-407.
8. S. Y. Hong, Y. M. Park, Y. H. Jang, B. H. Min and H. C. Yoon, *BioChip J.*, 2012, **6**, 213-220.
9. A. C. Bay-Jensen, Q. Liu, I. Byrjalsen, Y. Li, J. Wang, C. Pedersen, D. J. Leeming, E. B. Dam, Q. Zheng, P. Qvist and M. A. Karsdal, *Clin. Biochem.*, 2011, **44**, 423-429.
10. S. Gargiulo, P. Gamba, G. Poli and G. Leonarduzzi, *Curr. Pharm. Des.*, 2014, **20**, 2993-3018.
11. E. Steck, S. Breit, S. J. Breusch, M. Axt and W. Richter, *Biochem. Biophys. Res. Commun.*, 2002, **299**, 109-115.
12. T. Knorr, F. Obermayr, E. Bartnik, A. Zien and T. Aigner, *Ann. Rheum. Dis.*, 2003, **62**, 995-998.
13. A. Ranok, P. Khunkaewla and W. Suginta, *Monoclon. Antib. Immunodiagn. Immunother.*, 2013, **32**, 317-325.
14. S. Y. Song, Y. D. Han, S. Y. Hong, K. Kim, S. Y. Yang, B. H. Min and H. C. Yoon, *Anal. Biochem.*, 2012, **420**, 139-146.
15. Y. M. Park, S. J. Kim, K. J. Lee, S. S. Yang, B. H. Min and H. C. Yoon, *Biosens. Bioelectron.*, 2015, **67**, 192-199.
16. Y. Sun, X. Hu, Y. Zhang, J. Yang, F. Wang, Y. Wang, R. Deng and G. Zhang *J. Agric. Food Chem.*, 2014, **62**, 11116-11121.
17. W. Chaocharoen, W. Suginta, W. Limbut, A. Ranok, A. Numnuam, P. Khunkaewla, P. Kanatharana, P. Thavarungkul and A. Schulte, *Bioelectrochem.* 2015, **101**, 106-113.
18. C. Berggren, B. Bjarnason and G. Johannsson, *Electroanalysis*, 2001, **13**, 173-180.
19. C. Berggren and G. Johannsson, *Anal. Chem.* 1997, **69**, 3651-3657.
20. W. Limbut, P. Kanatharana, B. Mattiasson, P. Asawatreratanakul and P. Thavarungkul, *Biosens. Bioelectron.*, 2006, **22**, 233-240.
21. M. Schimpl, C. L. Rush, M. Betou, I. M. Eggleston, A. D. Recklies and D. M. F. Van Aalten, *Biochem. J.*, 2012, **44**, 149-157.

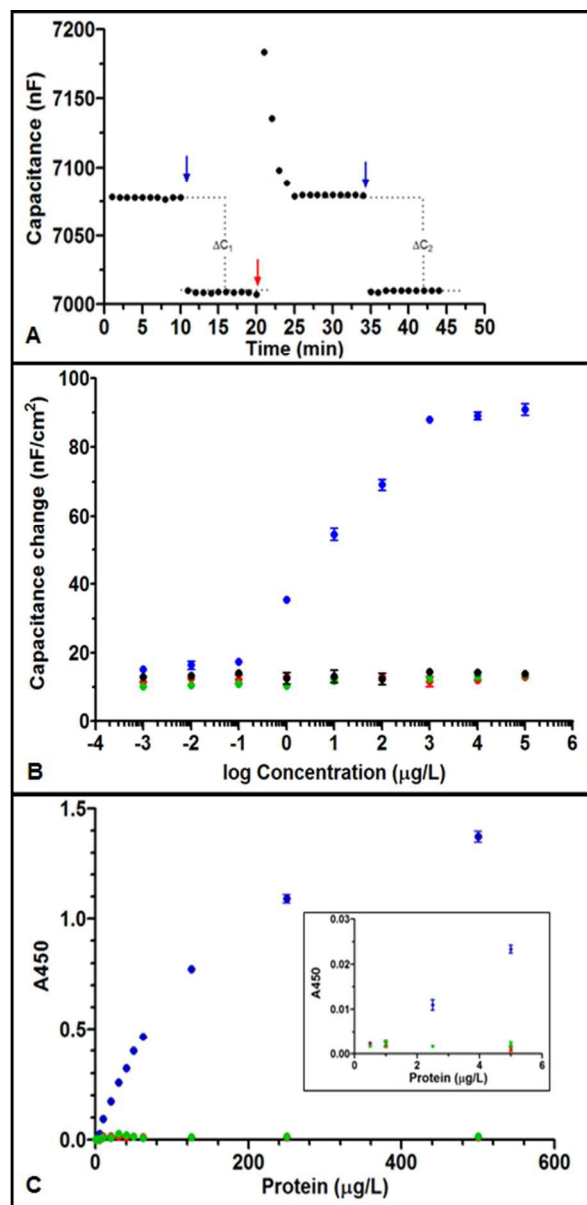


Fig 1. (A) Capacitance response of anti-hYKL-39-modified electrode. The baseline signal of the carrier buffer is initially recorded. 1st injection of 100 $\mu\text{g/L}$ of hYKL-39 (left blue arrow) triggered antigen binding and a decrease of capacitance (ΔC_1). Injection of the regeneration buffer (red arrow) removed hYKL-39 from the immunosensor surface and the capacitance returned to initial baseline. 2nd injection of 100 $\mu\text{g/L}$ of hYKL-39 (right blue arrow) produced capacitance change ΔC_2 . (B) Concentration dependence of the capacitance change for a hYKL-39 immunosensor elicited by hYKL-39 (blue curve) and hYKL-40 (red curve) and hAMCase (green curve) exposure. (C) Enzyme-linked immunosorbent assay (ELISA) of hYKL-39. Binding of anti-hYKL-39 IgG (50 μL , 15 $\mu\text{g/L}$) to different amounts of immobilized hYKL-39 (blue trace), hYKL-40 (red trace) and hAMCase (green trace). The inset is a zoom of the signal response at low concentration of the antigens.

130x266mm (96 x 96 DPI)

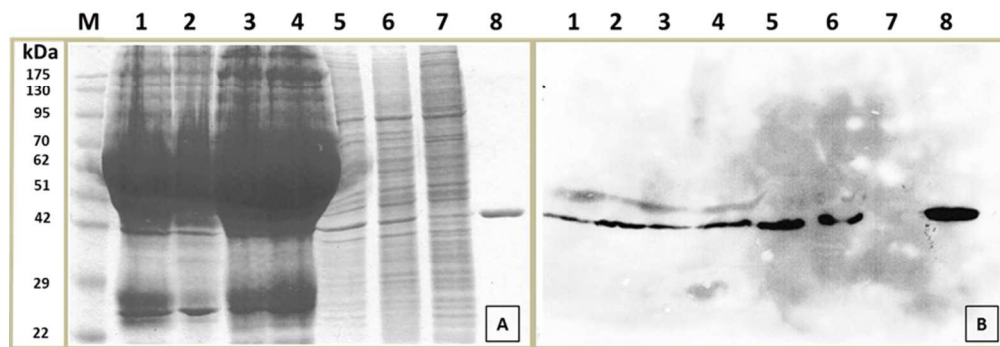


Fig 2. Clinical samples and cell lysate electrophoresis on a 10% polyacrylamide-SDS gel. Lane: M, protein markers; lanes 1 – 4, synovial fluid from osteoarthritis patients; lane 5, Jurkat cell lysate; lane 6, U937 cell lysate; lane 7, 293t cell lysate; lane 8, pure hYKL-39 (2 μ g). (A) Coomassie-blue stained gel. (B) Immunoblot detected with anti-hYKL-39 polyclonal antibody (1:10,000 dilution).
248x88mm (96 x 96 DPI)

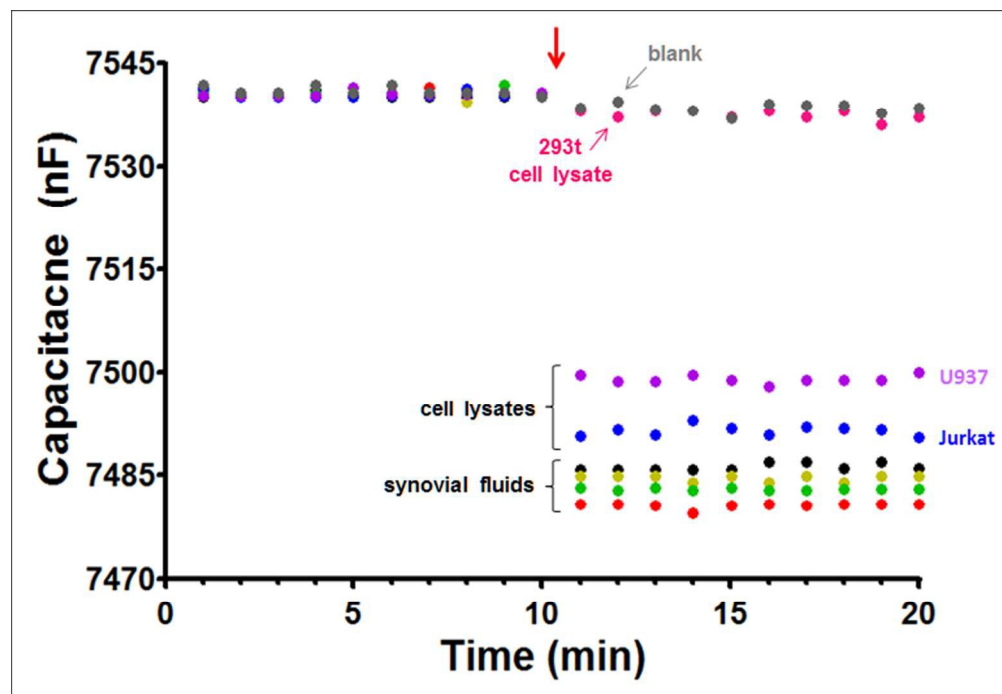


Fig 3. Cell lysate and synovial fluid analysis, by capacitive immunosensing. Sample injection is marked by a red arrow. A decrease in the sensor capacitance indicates the presence of hYKL-39, the concentration of which can be determined from the calibration curve.
203x140mm (96 x 96 DPI)

YKL-39 concentration ($\mu\text{g/L}$)	Detected hYKL-39 concentration ($\mu\text{g/L}$)			
	Immunosensor	% recovery	ELISA	% recovery
0.5	0.5 ± 0.1	103.9 ± 1.4	n. d.	n. d.
2.5	2.6 ± 0.1	100.7 ± 1.1	2.5 ± 0.6	99.9 ± 2.2
5.0	5.1 ± 0.1	100.4 ± 3.8	5.1 ± 0.1	101.5 ± 2.6
50.0	51.2 ± 0.3	102.4 ± 0.6	49.6 ± 1.5	99.1 ± 3.0
150.0	149.9 ± 2.4	100.0 ± 1.6	96.4 ± 0.6	64.3 ± 0.4

Table 1: Determination of hYKL-39 in model samples using capacitive immunosensor (n=3) and standard ELISA (n=3) quantification
249x77mm (150 x 150 DPI)

Sample	Detected hYKL-39 concentration ($\mu\text{g/L}$)	
	Immunosensor	ELISA
Synovial fluid # 1	59.4 \pm 2.4	58.3 \pm 3.4
Synovial fluid # 2	106.3 \pm 0.8	107.0 \pm 2.5
Synovial fluid # 3	68.1 \pm 1.3	67.7 \pm 1.2
Synovial fluid # 4	89.0 \pm 2.7	88.8 \pm 1.6
Jurkat	26.4 \pm 0.4	25.2 \pm 3.1
U937	10.6 \pm 0.3	9.8 \pm 0.8
293t	n. d.	n. d.

n. d. = not detected

Table 2: Determination of hYKL-39 in clinical samples and cell lysates using capacitive immunosensor (n=3) and standard ELISA (n=3) quantification
220x126mm (96 x 96 DPI)

Spiked concentration ($\mu\text{g/L}$)	Detected concentration ($\mu\text{g/L}$)			
	Immunosensor ($\mu\text{g/L}$)	Recovery (%)	ELISA ($\mu\text{g/L}$)	Recovery (%)
Synovial fluid#1 + 50 $\mu\text{g/L}$	109.1 \pm 0.1	99.1 \pm 0.1	110.6 \pm 1.2	101.1 \pm 1.2
Synovial fluid#2 + 50 $\mu\text{g/L}$	155.1 \pm 1.0	99.2 \pm 0.6	156.7 \pm 0.8	99.8 \pm 0.4
Synovial fluid#3 + 50 $\mu\text{g/L}$	118.4 \pm 0.6	100.3 \pm 0.5	118.7 \pm 1.2	100.8 \pm 0.8
Synovial fluid#4 + 50 $\mu\text{g/L}$	139.6 \pm 0.4	100.4 \pm 0.3	141.6 \pm 1.2	102.0 \pm 0.7
293t + 20 $\mu\text{g/L}$	20.2 \pm 0.4	100.8 \pm 2.2	20.5 \pm 0.5	102.4 \pm 1.8
293t + 30 $\mu\text{g/L}$	29.7 \pm 0.2	99.1 \pm 0.7	30.4 \pm 0.5	101.2 \pm 1.2

Table 3: Determination of hYKL-39 in spiked clinical samples and 293t cell lysate using capacitive immunosensor (n=3) and standard ELISA (n=3) quantification
249x100mm (96 x 96 DPI)